Electronic structure effects on B K-edge XANES of minerals

Ondřej Šipr[a]* and Francesco Rocca[b]

[a]Institute of Physics of the ASCR v.v.i., Cukrovarnická 10, CZ-162 53 Prague, Czech Republic, and [b]Istituto di Fotonica e Nanotecnologie del CNR, Sezione 'FBK-CeFSA' di Trento, Via alla Cascata 56/C, I-38123 Povo (Trento), Italy. E-mail: sipr@fzu.cz

In order to assess the usability of X-ray absorption near-edge structure (XANES) for studying the structure of BO_n-containing materials, the dependence of theoretical XANES at the B K-edge on the way the scattering potential is constructed is investigated. Real-space multiple-scattering calculations are performed for self-consistent and non-self-consistent potentials and for different ways of dealing with the core hole. It is found that in order to reproduce the principal XANES features it is sufficient to use a non-self-consistent potential with a relaxed and screened core hole. Employing theoretical modelling of XANES for studying the structure of boron-containing glasses is thus possible. The core hole affects the spectrum significantly, especially in the pre-edge region. In contrast to minerals, B K-edge XANES of BPO_4 can be reproduced only if a self-consistent potential is employed.

Keywords: B K-edge XANES; borate glasses; minerals.

1. Introduction

X-ray absorption spectroscopy of solids probes unoccupied electron states in an element- and angular-momentum-specific way. Depending on the energy of the excited photoelectron, the X-ray absorption spectrum is often divided into the X-ray absorption near-edge structure (XANES) and the extended X-ray absorption fine structure (EXAFS). The EXAFS spectroscopy can be conveniently described in terms of backscattering from neighbouring atoms and has become a powerful tool for studying local structure. On the other hand, XANES spectroscopy is not routinely used for structural studies. The main reason is the complexity of the processes which underlie XANES spectra, meaning that extracting structural information from the data is difficult and possibly ambiguous. Besides, the accuracy of theoretical modelling is still significantly lower for XANES than for EXAFS. Despite this, there has been a lot of effort to use also the XANES part of the spectrum for studying the atomic structure. This is mainly because, for some materials, it is very difficult to resolve very faint EXAFS oscillations in the experiment while the XANES spectrum can be recorded under much more general circumstances. Apart from that, XANES may contain information not accessible by standard EXAFS analysis, such as bond angles.

Several approaches to extract structural information from XANES have been tested and employed. Mostly, they are based either on 'fingerprinting' (*i.e.* on identifying spectral features characteristic for certain geometric arrangements) (Farges *et al.*, 1997; Šipr, 2002) or on comparing spectra

calculated for trial structures with experiment (Benfatto *et al.*, 2003; Šipr *et al.*, 2004). In both approaches one has to distinguish which spectral features are sensitive to atomic arrangements and which spectral features are associated with the details of the electronic structure (which enters the calculation *via* scattering potentials). These two aspects cannot be strictly separated because the electronic structure is determined by the atomic arrangement which, in turn, has to be such that the total energy of the system is minimized and in this way it again depends on the electronic structure. Nevertheless, one can often identify some features in the XANES spectra which are especially sensitive to changes in the arrangement of atoms and hence can be indicative of the atomic structure, and other features which are more sensitive to the electronic structure and their usability in structural studies is, therefore, limited.

A class of systems where a lot of effort has been devoted to structural studies represent borate and borosilicate glasses and melts. Learning more about the short-range and medium-range order around B atoms in these systems is desirable, so that studies linking their properties and structure could proceed further (Dalba & Wright, 2008). When studying the structure of glasses, it is often convenient to start with a related compound for which the structure is known. In the case of borate glasses, boron-containing minerals seem to be a reasonable choice for the starting point: in both cases the B atoms are, namely, coordinated by three or four oxygen atoms. On the other hand, borate glasses contain a continuous network of B—O bonds, while minerals can contain isolated BO_n units within their crystallographic structures. This means

that the analogy between glasses and minerals could be useful for studying the short-range order around B atoms but caution should be taken when studying the medium-range order.

Recent studies showed that B K-edge XANES of minerals containing BO_n (n = 3, 4) units is probably dominated by the atomic arrangement: spectra generated at the BO_3 units are characterized by an intensive sharp peak followed by a broader peak about 10 eV above it, while spectra generated at the BO_4 units are characterized by a single peak positioned in energy between the peaks associated with the BO_3 units (Garvie *et al.*, 1995; Kasrai *et al.*, 1998; Fleet & Muthupari, 2000; Fleet & Liu, 2001). This suggests that the B K-edge XANES might be useful for studying local structure around B atoms. Having an experimental method to detect the relative abundance of tri- or tetra-coordinated boron is highly desirable, because B atoms are incorporated in networks which underlie the structure of several types of glasses. Nuclear magnetic resonance (NMR) spectra of ^{11}B proved to be very useful in determining the ratio of B atoms occurring in BO_3 and BO_4 environments (Bray, 1992). It would be useful, nevertheless, to have an independent method of measuring this quantity and possibly to probe not only the short-range order but also the medium-range order. Moreover, NMR cannot be used in situations where the content of boron is very small, such as in thin films or in materials where boron is the dopant. The possibility of using B K-edge XANES for determining the ratio of BO_3 and BO_4 units was explored in several studies (Sauer *et al.*, 1993; Li *et al.*, 1995; Fleet & Muthupari, 1999; Carboni *et al.*, 2003; Šipr *et al.*, 2006). The potential of XANES spectroscopy to investigate medium-range order around B atoms was studied as well (Šipr *et al.*, 2007). Measuring B K-edge absorption spectra is quite challenging because of several inherent difficulties. Despite that, several experiments on B K-edge XANES of borate glasses were performed recently (Ide *et al.*, 2006; Handa *et al.*, 2006; Yang *et al.*, 2006).

In the past years the present authors have investigated the possibility of employing XANES spectra simulations for studying the structure of boron-containing materials; the focus was on analyzing the results in terms of peaks positions and intensities, with B atoms located in various crystallographic positions (Šipr *et al.*, 2006, 2007). The purpose of this paper is to further investigate the influence of scattering potentials on the calculated B K-edge XANES. Our particular aims include (i) verifying whether self-consistent potentials have to be involved for a successful reproduction of the experimental spectra of minerals, and (ii) evaluating various ways of dealing with the core hole created by the photoabsorption. Performing such a study is important because only those XANES features which are sufficiently robust to the way the potential is constructed can be employed in structural studies of systems with unknown structure.

Based on previous works on XANES of various materials, one can expect that using a non-self-consistent potential constructed *via* the Mattheiss prescription should be appropriate for reproducing the gross features of XANES spectra. However, in some cases use of self-consistent potentials

proved to be necessary. Our earlier study showed that non-self-consistent potentials are good enough to reproduce the principal difference between B K-edge spectra of BO_3 and BO_4 units (Šipr *et al.*, 2006); however, the agreement between theory and experiment was not perfect and it would be interesting to learn whether this can be remedied by use of self-consistent potentials.

A proper treatment of the core hole would require dealing with the dynamics of the excited photoelectron. Various schemes for this were designed but their broader use is still hindered by technical difficulties (Shirley, 1998, 2004; Schwitalla & Ebert, 1998; Ankudinov *et al.*, 2003). For routine use, approximating the core hole effect by a static scheme is still the most practical approach. Good agreement with experiment is often obtained by employing the final state approximation and treating the core hole as relaxed and screened, *i.e.* by transferring a $1s$ electron into the lowest unoccupied level and letting the electrons adjust to this (Rehr & Albers, 2000; Natoli *et al.*, 2003). The relaxed and screened model was used in a recent study of B K-edge XANES of borate glasses (Šipr *et al.*, 2006, 2007). Another scheme for treating the core hole has been called the '$(Z + 1)^{*}$' approximation; it was suggested on a semi-empirical basis specifically for boron and other low-Z elements and, reportedly, led to a better agreement between theoretical and experimental XANES than the final state approximation (Brydson *et al.*, 1988; Rowley *et al.*, 1990). On the other hand, angular-resolved B K-edge spectra of MgB_2 were reproduced successfully by a calculation where the core hole was not involved (Zhang *et al.*, 2003). A more detailed investigation of the core hole effect in B K-edge XANES is thus desirable.

We will show in the following sections that, in order to analyze B K-edge XANES of compounds with BO_n units, one can use calculations based on a non-self-consistent potential with a relaxed and screened core hole. Employing theoretical modelling of XANES for studying the structure of boron-containing glasses is thus possible.

2. Methods

2.1. Investigated materials

We investigated BO_3-containing minerals calciborite, ludwigite and vonsenite, BO_4-containing minerals danburite and datolite, and also BO_4-containing boron phosphate [because this compound had often been used as a reference (Kasrai *et al.*, 1998; Fleet & Muthupari, 2000)]. Boron atoms occupy unique crystallographic positions in these minerals, thus allowing a simple comparison between the observed and calculated spectra. Information about the local structure around B atoms is given in Table 1.

2.2. Computational framework

B K-edge XANES was calculated *ab initio* in real space *via* the multiple-scattering or Green function technique (Natoli *et al.*, 2003), using the *rsms* code (Šipr, 1996–1999; Vvedensky *et al.*, 1986). This approach is formally equivalent to other

Table 1
Local structure around B atoms in materials investigated in this work.

The third column contains the boron coordination number n, the fourth column contains the distances between B and its nearest neighbours, and the fifth column contains the reference to the original work from which the structure was taken.

Material	Composition	n	B—O distances (Å)	Structure
Calciborite	CaB_2O_4	3	1.33, 1.39, 1.40	Marezio *et al.* (1963)
Ludwigite	Mg_2FeBO_5	3	1.35, 1.35, 1.41	Mokeeva (1968)
Vonsenite	Fe_3BO_5	3	1.38, 1.38, 1.39	Swinnea & Steinfink (1983)
Boron phosphate	BPO_4	4	1.44, 1.44, 1.44, 1.44	Schulze (1934)
Danburite	$CaB_2Si_2O_8$	4	1.45, 1.46, 1.48, 1.50	Sugiyama & Takeuchi (1985)
Datolite	$CaBSiO_4OH$	4	1.46, 1.48, 1.49, 1.50	Foit *et al.* (1973)

approaches to solving the Schrödinger equation for unoccupied states (Natoli & Benfatto, 1986). Specifically, in comparison with the widely employed band-structure approach, our method deals not with infinite crystals but with finite clusters embedded in a sea of free electrons. On the one hand, this invokes an additional need to care about the convergence of the calculated spectra with the cluster size. On the other hand, use of finite clusters makes it more easier to account for the influence of the core hole (because translational symmetry is not required). Spectra presented in this work were obtained for quite large clusters of about 250 atoms; however, fairly well size-converged spectra have already been obtained for about 50 atoms (Šipr *et al.*, 2006).

The exchange and correlation effects were accounted for *via* an energy-independent $X\alpha$ potential. The agreement between the theoretical and experimental peaks positions would probably improve if an energy-dependent exchange-correlation potential was used. However, it is still quite difficult to decide *a priori* which form of the exchange-correlation potential would be most suitable for a particular situation (Chaboy & Quartieri, 1995; Ankudinov, 1999; Hatada & Chaboy, 2007). Therefore, we stick with the energy-independent $X\alpha$ potential which is sufficient for the purpose of this study. As concerns the value of the α parameter, we use $\alpha = 0.67$, as originally suggested by Kohn & Sham (1965). This is a compromise between the slightly larger values of α optimized for occupied states (Schwarz, 1972) and lower values which seem more appropriate for unoccupied states (Bugaev *et al.*, 1986). A muffin-tin approximation on the shape of the potential was imposed. Muffin-tin radii were set so that the initial superimposed potentials match at the touching points (or rather, as the matching condition cannot be strictly met for all the atoms, so that the overall difference is minimal), allowing for an overlap of at most 5%. The muffin-tin zero was identified with the average of the interstitial potential V_{int}. In this way it deviates, on average, less from the 'true' non-muffin-tin potential than it does in the case when the muffin-tin zero is identified with the value of the intra-sphere potential at the sphere boundary. Our choice is also motivated by our previous experience with XANES of oxides (see, for example, Šipr *et al.*, 1999*b*).

Our formalism accounts for transitions only to states forming the continuum spectrum above the muffin-tin zero. Weakly bound states above V_{int} will show up as resonances (extended continuum framework).

Two kinds of potential construction were employed. (i) A non-self-consistent muffin-tin potential was constructed according to the Mattheiss prescription (superposition of potentials and charge densities of isolated atoms). (ii) A self-consistent muffin-tin potential was constructed by means of SCF-$X\alpha$ molecular-like calculations (Johnsson, 1973) performed for clusters of 20–30 atoms embedded in an infinite crystal, using an improved *xascf* code (Cook & Case, 1980; Šipr *et al.*, 1999*a*; Šipr & Šimůnek, 2001).

Three models of dealing with the core hole were tested. In the first model the core hole was completely ignored, *i.e.* the XANES calculations were made for a ground-state potential. The second approach is referred to as a relaxed and screened model: a $1s$ electron is moved from the core level into the lowest unoccupied level and the electrons are then allowed to relax. The third model is the semi-empirical $(Z + 1)^*$ approximation suggested by Brydson *et al.* (Garvie *et al.*, 1995; Brydson *et al.*, 1988; Rowley *et al.*, 1990). It consists of substituting the photoabsorbing atom with an atom next to it in the periodic table (in our case taking C instead of B), moving a $1s$ electron from the core level into the lowest unoccupied level and allowing the electrons to relax.

The raw calculated spectra were broadened by an energy-dependent Lorentzian to simulate the combined effect of the experimental resolution, of the decay of the core hole and of the decay of the excited photoelectron. The constant part of the broadening was set to 0.40 eV, the energy-dependent part of the broadening was set by amending the 'universal curve' (Müller *et al.*, 1982) according to the suggestions of Benfatto *et al.* (2003) so that a good agreement between theory and experiment is achieved (we used damping associated with four valence electrons, starting at energy $E_s = 5$ eV).

When calculating a XANES spectrum, one has to include only those electron states which are above the onset of unoccupied states (Fermi level in the case of metals). When using non-self-consistent potentials, we do not perform the band-structure calculations, meaning that the threshold energy has to be set by hand. When constructing self-consistent potentials, we obtain electron states for clusters of 20–30 atoms embedded in a solid, so the threshold energy obtained thereby may differ by a few electronvolts from the threshold energy that would be obtained for (infinite) crystals. Therefore, there is always some ambiguity in setting of the onset of XANES. The established procedure is to put the threshold energy in a position which corresponds to some deep minimum in the density of states so that a reasonable agreement between theoretical and experimental XANES is obtained. The exact location of this onset may be subject to debate, especially if the agreement between the theory and the experiment is not perfect. That is also the case of some theoretical XANES spectra presented in §3 (especially those obtained *via* non-self-consistent potentials). Nevertheless, our conclusions do not depend on any particular choice of the threshold energy; they would remain the same even if these

onset energies varied within several electronvolts in comparing experiments with theory.

3. Results

3.1. Influence of self-consistency in potentials

A comparison between theoretical and experimental B K-edge XANES for materials containing BO_3 units is shown in the left-hand panels of Fig. 1, and a comparison for materials containing BO_4 units is shown in the right-hand panels. The theoretical spectra were obtained for non-self-consistent potentials and for self-consistent potentials; the core hole was included *via* the relaxed and screened model. Experimental B K-edge XANES spectra of ludwigite, vonsenite, danburite and datolite are from Fleet & Muthupari (2000), the experimental spectrum of calciborite is from Fleet & Liu (2001), and the experimental spectrum of BPO_4 is from Šipr *et al.* (2006).

The vertical scale of the spectra was set so that the intensities of the main peaks match. The horizontal alignment was set so that the best overall agreement between experiment and theory is achieved. The origin of the energy scale is arbitrary; our theoretical scheme does not provide accurate absolute energies of the absorption edges. One should also note that the original experimental spectra taken from the literature display some disagreement in the absolute energy scale, owing to different calibration of the beamlines.

One can see from Fig. 1 that, in most cases, self-consistency in the potential does not have a major impact on the calculated XANES. In particular, the distinction between the general shapes of spectra of minerals with BO_3 units and with BO_4 units is well reproduced for both types of potential. The biggest improvement caused by employing self-consistent potentials occurs at the pre-peak of BO_3-containing minerals: its intensity is reproduced correctly only if a self-consistent potential is used. Calculation with a non-self-consistent potential is able to predict the existence of the pre-peak but fails to reproduce its intensity. A specific situation occurs for the B K-edge XANES of BPO_4, which cannot be reproduced even in its gross form unless a self-consistent potential is used.

In Fig. 1 we should note that in the experimental XANES of danburite and (to a lesser degree) of datolite there is a small pre-peak at $E \simeq 4\,\text{eV}$ that is attributed to B in BO_3 units which are created in the sample because of radiation damage (Garvie *et al.*, 1995; Kasrai *et al.*, 1998). A similar pre-peak was observed also in earlier measurements of the B K-edge XANES of BPO_4 (Kasrai *et al.*, 1998; Fleet & Muthupari, 2000). As demonstrated by Kasrai *et al.*, also on that occasion the peak was produced by some surface radiation damage [*cf*. Fig. 3A in Kasrai *et al.* (1998)]. We were able to eliminate this spurious peak in a more recent experiment at ELETTRA (Italy) (Šipr *et al.*, 2006), so this last experimental spectrum is presented here as a reference for BPO_4.

Figure 1
Theoretical B K-edge XANES of boron-containing compounds obtained using self-consistent potentials (solid lines) and using non-self-consistent potentials (broken lines), compared with experiment (dotted lines). Results for compounds with BO_3 units are in the left-hand panels, results for compounds with BO_4 units are in the right-hand panels. A core hole is always included (within the relaxed and screened model). The origin of the energy scale is arbitrary.

3.2. Core hole effect

The influence of the core hole is demonstrated in Fig. 2 where we show B K-edge XANES calculated for self-consistent potentials generated (i) without the core hole and (ii) with the
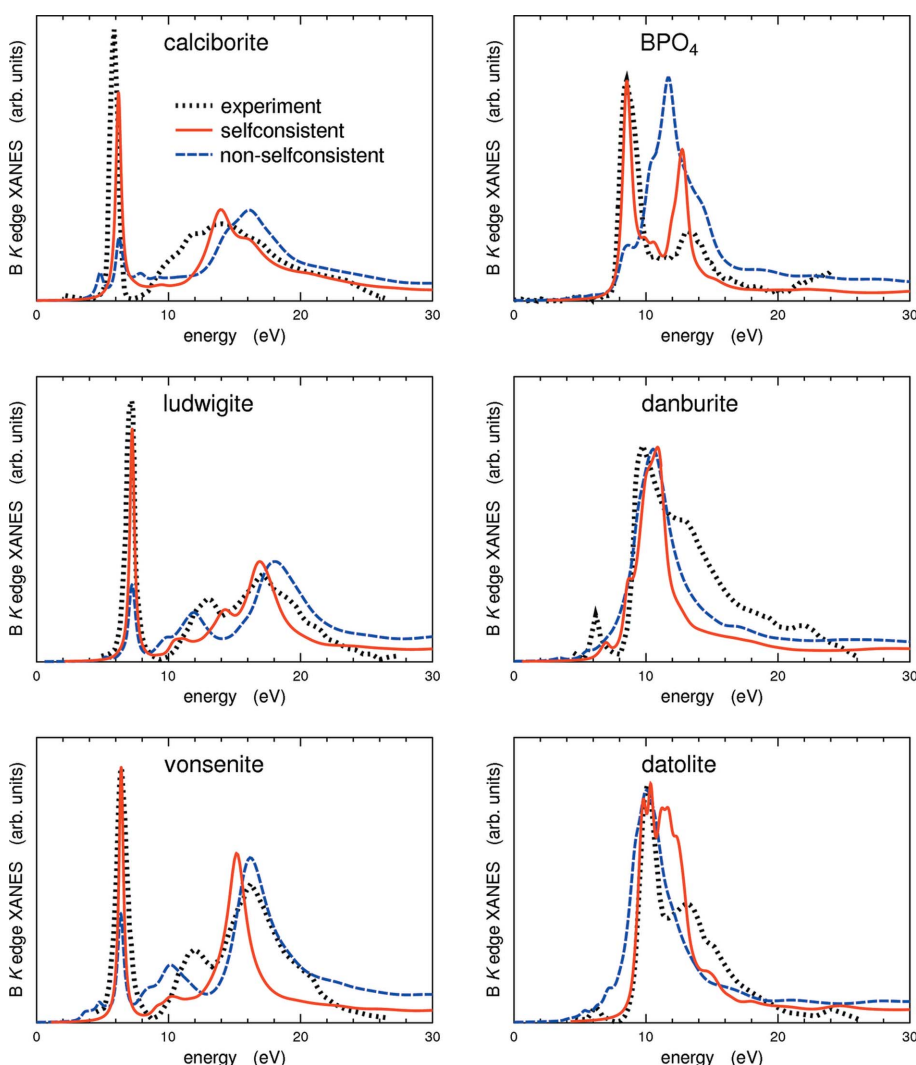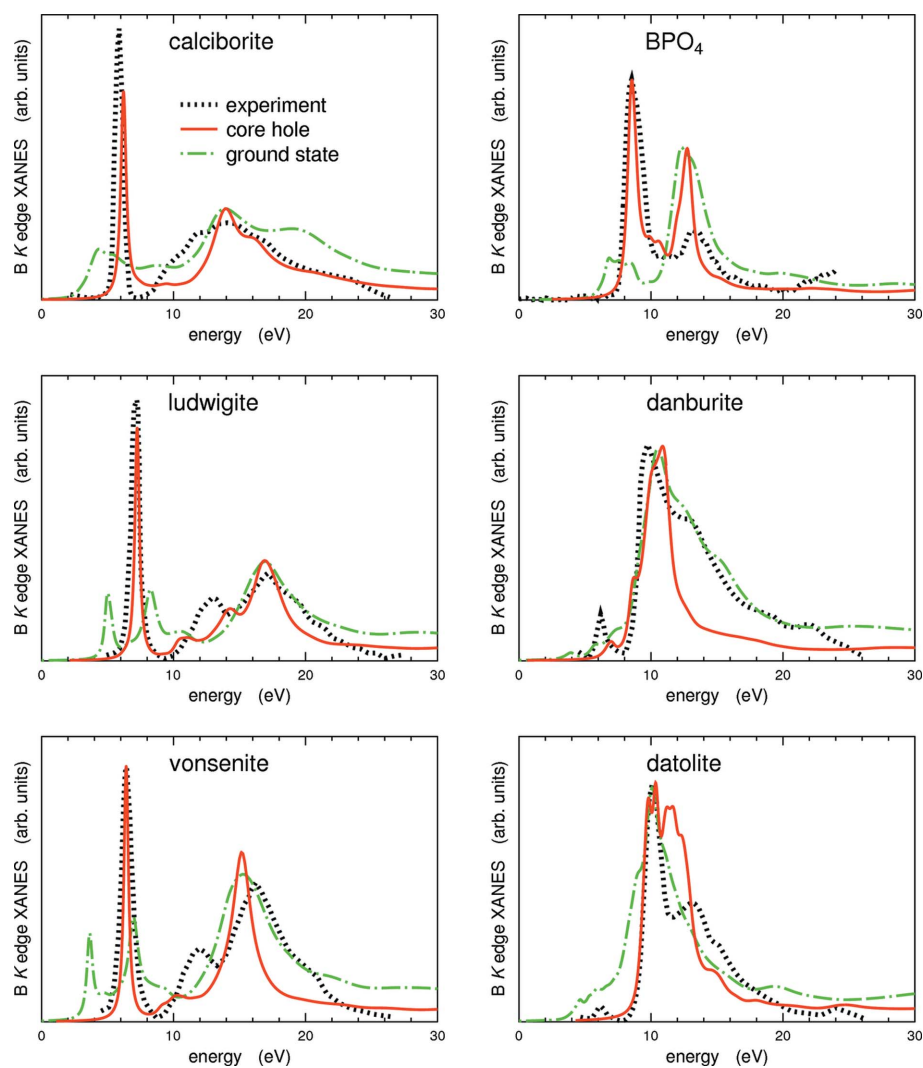
Figure 2
Theoretical B *K*-edge XANES of boron-containing compounds obtained when the core hole is taken into account within the relaxed and screened model (solid lines) and when the core hole is neglected (chain lines). Experimental spectra are shown *via* dotted lines. All the calculations were performed for self-consistent potentials. The origin of the energy scale is arbitrary.

in Fig. 3. The case of non-self-consistent potentials is highlighted here, because that is the situation where the $(Z + 1)^*$ scheme is most likely to be used.
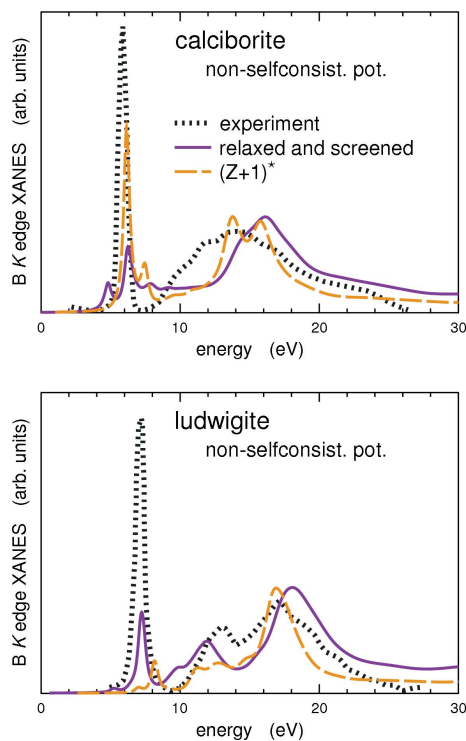
It is evident from Fig. 3 that in some cases the $(Z + 1)^*$ scheme enhances the intensity of the pre-peak and thus improves the agreement between theory and experiment (calciborite) while in other cases it worsens the agreement (ludwigite). This is our general experience with the $(Z + 1)^*$ scheme, drawn also from results obtained for other compounds as well as for self-consistent potentials (we do not show all the results here for brevity): sometimes the $(Z + 1)^*$ scheme helps but sometimes it harms, and the outcome seems to be, at present, unpredictable.

4. Discussion

Our main objective was to find out whether the main difference between the B *K*-edge XANES of BO_3-containing and BO_4-containing minerals can be reproduced by calculations based on non-self-consistent potentials. Our second objective was to assess the suitability of various models of incorporating the core hole. We found that by using non-self-consistent potentials the gross features of spectra of BO_n-containing minerals can indeed be reproduced. However, in order to obtain the correct intensity of the pre-peak of minerals with BO_3 units, self-consistency has to be involved. The core hole plays an important role in B *K*-edge XANES, especially close to the edge. Its influence can be fairly well described by the relaxed and screened model.

Our finding that non-self-consistent and self-consistent potentials give rise to similar spectra is plausible. Non-self-consistent potentials proved to be quite efficient in XANES calculations in the past. Typically, using self-consistent potential affects the calculated XANES by the same degree as changing the exchange-correlation potential (self-energy) or details of muffin-tin potential construction (Rehr & Albers, 2000; Ankudinov, 1999). Self-consistency improves the quantitative agreement between theory and experiment but usually it is not necessary for reproducing the most characteristic features of the spectra. From this perspective, the fact that using a self-consistent potential is necessary for reproducing even the gross features of B *K*-edge XANES of BPO_4 is striking and surprising (see upper right panel of Fig. 1). It is noteworthy that BPO_4 differs from boron-containing minerals

core hole included within the relaxed and screened model. One can see that inclusion of the core hole modifies the calculated spectrum significantly. In particular, it has to be included in order to reproduce the pre-edge peak in the BO_3-containing minerals accurately. A similar situation occurs for the first peak of BPO_4. At higher photoelectron energies the influence of the core hole is smaller. On the other hand, for danburite the agreement between theory and experiment is better without the core hole. For datolite it is difficult to choose between the two models (the agreement is not very good for either of them).

Finally, we explore further how the calculated spectra depend on the way the core hole is included, with special focus on the semi-empirical $(Z + 1)^*$ scheme (Brydson *et al.*, 1988). For each of the compounds, we calculated the B *K*-edge XANES with the core hole included not only *via* the relaxed and screened model but also *via* the $(Z + 1)^*$ scheme. As an illustration, results for calciborite and ludwigite are presented

Figure 3
B K-edge XANES of calciborite (upper panel) and ludwigite (lower panel) calculated for two different ways of accounting for the core hole: either it is included using the relaxed and screened model (solid lines) or it is included using the $(Z + 1)^*$ scheme (broken lines). Non-self-consistent potentials were employed. Experimental spectra are shown *via* dotted lines. The origin of the energy scale is arbitrary.

also from another point of view: namely, B K-edge XANES of BPO_4 is dominated by long-range order while XANES of minerals is dominated by short-range order (Šipr *et al.*, 2006). The BPO_4 is thus not a good reference compound for studying B K-edge XANES of boron-containing minerals or glasses.

The largest improvement in XANES caused by using self-consistent potential occurs at the pre-peak (see Fig. 1). Similar observations were made earlier for other compounds such as, for example, CuO (Šipr & Šimůnek, 2001). The changes in B K-edge XANES caused by using self-consistent or non-self-consistent potential are, nevertheless, smaller than changes that would be caused by varying the local geometry. This issue was dealt with in our earlier work on glasses (Šipr *et al.*, 2004, 2007; Kuzmin *et al.*, 2006) and on minerals (Šipr *et al.*, 2006).

Concerning the core hole, we found that accounting for it is necessary to achieve a good agreement with experiment, especially for systems with tri-coordinated boron, and that its influence can be described *via* the relaxed and screened model. Similar conclusions can be drawn from earlier studies of B K-edge XANES of TiB_2 (Lie *et al.*, 1999) and BN (Shirley, 2000; Jayawardane *et al.*, 2001). On the other hand, for MgB_2 the situation is not so clear: one study found that the polarization-dependence of B K-edge XANES of MgB_2 can be reproduced theoretically by ignoring the core hole (Zhang *et al.*, 2003) while another study, dealing with electron energy loss spectra, found that calculation with half of a (relaxed and screened) core hole leads to the best results (Jiang *et al.*, 2003).

One should note that the main difference between the above-mentioned studies rests in the treatment of the core hole and not in the particular technique of XANES calculation. It seems therefore that the importance and character of the 1s core hole differs from one compound to another.

Our results suggest that the $(Z + 1)^*$ approach, which was found to be helpful in B K-edge XANES of rhodizite and vonsenite (Brydson *et al.*, 1988; Rowley *et al.*, 1990), does not lead to a consistent improvement with respect to the relaxed and screened model. In any case, it is evident that the core hole affects B K-edge spectra in a significant way.

Although our calculations reproduce the principal difference between the spectra of minerals with BO_3 and BO_4 units, the agreement between theory and experiment is still not perfect. On the theory side, one of the reasons for the discrepancies could be the muffin-tin approximation (the structures of the minerals are not compact, meaning that having a constant interstitial potential could be a poor approximation). Another reason for the failure of the theory could be an inadequate treatment of the core hole: because the core hole has a significant influence on the spectra, deficiencies of its treatment might account for some of the difference between theory and experiment. Possibly, treating the sharp pre-peaks as bound states might improve calculated spectra in this area.

Possible reasons for the disagreement lie also on the side of the experiment. The measured samples were natural minerals (Fleet & Muthupari, 2000; Fleet & Liu, 2001) so they could slightly differ from the ideal structures we used in the calculations; the samples might contain defects, impurities, disorder. In fact, the presence of disorder is sometimes reflected already in the chemical formulas: *e.g.* while we assumed in our calculations that the composition of ludwigite is Mg_2FeBO_5, the original reference (Mokeeva, 1968) considered $(Mg_{1.85}Fe_{0.15})(Fe_{0.60}Al_{0.40})BO_5$. Besides, radiation-induced damage of the samples also plays a role (Garvie *et al.*, 1995; Kasrai *et al.*, 1998). So it is likely that at least part of the disagreement between theoretical and experimental curves in Fig. 1 is due to the fact that the calculations and measurements were actually performed for not quite identical materials.

In order to use X-ray absorption spectroscopy for studying the structure of boron-containing glasses and melts efficiently, *ab initio* calculations have to be involved. In these calculations, self-consistent potentials often cannot be used simply because the full structure is not known and hence, in principle, it is not possible to create a potential which would describe the situation perfectly. The present work implies that in these cases one can rely on calculations performed for non-self-consistent potentials, provided that a relaxed and screened core hole is included; it is just necessary to bear in mind that the intensity of the pre-peak will be underestimated.

5. Conclusions

In order to analyze B K-edge XANES of compounds with BO_n units, one can use calculations based on a non-self-consistent potential with a relaxed and screened core hole.

The core hole affects the spectrum significantly, especially in the pre-edge region. In contrast to the minerals, B K-edge XANES of BPO_4 can be reproduced only if self-consistent potentials are employed.

References

Ankudinov, A. L. (1999). *J. Synchrotron Rad.* **6**, 236–238.

Ankudinov, A., Nesvizhskii, A. I. & Rehr, J. J. (2003). *Phys. Rev. B*, **67**, 115120.

Benfatto, M., Della Longa, S. & Natoli, C. R. (2003). *J. Synchrotron Rad.* **10**, 51–57.

Bray, P. J. (1992). *Borate Glasses, Crystals and Melts*, edited by A. C. Wright, S. A. Feller and A. C. Hannon, p. 1. Sheffield: The Society of Glass Technology.

Brydson, R., Vvedensky, D. D., Engle, W., Sauer, H., Williams, B. G., Zeitler, E. & Thomas, J. M. (1988). *J. Phys. Chem.* **92**, 962–966.

Bugaev, L. A., Gegusin, I. I., Datsyuk, V. N., Novakovich, A. A. & Vedrinskii, R. V. (1986). *Phys. Status Solidi B*, **133**, 195–202.

Carboni, R., Pacchioni, G., Fanciulli, M., Giglia, A., Mahne, N., Pedio, M., Nannarone, S. & Boscherini, F. (2003). *Appl. Phys. Lett.* **83**, 4312–4314.

Chaboy, J. & Quartieri, S. (1995). *Phys. Rev. B*, **52**, 6349–6357.

Cook, M. & Case, D. A. (1980). *xascf.* Quantum Chemistry Program Exchange, Indiana University, Bloomington, IN, USA.

Dalba, G. & Wright, A. C. (2008). Editors. *Borate Glasses, Crystals and Melts.* Sheffield: The Society of Glass Technology.

Farges, F., Brown Jr, G. E. & Rehr, J. J. (1997). *Phys. Rev. B*, **56**, 1809–1819.

Fleet, M. E. & Liu, X. (2001). *Phys. Chem. Miner.* **28**, 421–427.

Fleet, M. E. & Muthupari, S. (1999). *J. Non-Cryst. Solids*, **255**, 233–241.

Fleet, M. E. & Muthupari, S. (2000). *Am. Mineral.* **85**, 1009–1021.

Foit, F. F., Phillis, M. W. & Gibbs, G. V. (1973). *Am. Mineral.* **58**, 909–914.

Garvie, L. A. J., Craven, A. J. & Brydson, R. (1995). *Am. Mineral.* **80**, 1132–1144.

Handa, K., Ide, J., Nishioyama, Y., Ozutsumi, K., Dalba, G., Ohtori, N. & Umesaki, N. (2006). *Phys. Chem. Glasses: Eur. J. Glass Sci. Technol. B*, **47**, 445–447.

Hatada, K. & Chaboy, J. (2007). *Phys. Rev. B*, **76**, 104411.

Ide, J., Ozutsumi, K., Handa, K., Dalba, G., Ohtori, N. & Umesaki, N. (2006). *Phys. Chem. Glasses: Eur. J. Glass Sci. Technol. B*, **47**, 521–523.

Jayawardane, D. N., Pickard, C. J., Brown, L. M. & Payne, M. C. (2001). *Phys. Rev. B*, **64**, 115107.

Jiang, B., Jiang, N. & Spence, J. (2003). *J. Phys. Condens. Matter*, **15**, 1299–1304.

Johnsson, K. H. (1973). *Adv. Quant. Chem.* **7**, 143–185.

Kasrai, M., Fleet, M. E., Muthupari, S., Li, D. & Bancroft, G. M. (1998). *Phys. Chem. Mineral.* **25**, 268–272.

Kohn, W. & Sham, L. J. (1965). *Phys. Rev.* **140**, A1133–A1138.

Kuzmin, A., Dalba, G., Fornasini, P., Rocca, F. & Šipr, O. (2006). *Phys. Rev. B*, **73**, 174110.

Li, D., Bancroft, G. M., Fleet, M. E., Hess, P. C. & Yin, Z. F. (1995). *Am. Mineral.* **80**, 873–877.

Lie, K., Brydson, R. & Davock, H. (1999). *Phys. Rev. B*, **59**, 5361–5367.

Marezio, M., Plettinger, H. A. & Zachariasen, W. H. (1963). *Acta Cryst.* **16**, 390–392.

Mokeeva, V. I. (1968). *Geochem. Int.* **5**, 809–813.

Müller, J. E., Jepsen, O. & Wilkins, J. W. (1982). *Solid State Commun.* **42**, 365–368.

Natoli, C. R. & Benfatto, M. (1986). *J. Phys. Colloq.* **47**, C8-11–C8-23.

Natoli, C. R., Benfatto, M., Della Longa, S. & Hatada, K. (2003). *J. Synchrotron Rad.* **10**, 26–42.

Rehr, J. J. & Albers, R. C. (2000). *Rev. Mod. Phys.* **72**, 621–654.

Rowley, P. N., Brydson, R., Little, J. & Saunders, S. R. (1990). *Philos. Mag. B*, **62**, 229–238.

Sauer, H., Brydson, R., Rowley, P. N., Engel, W. & Thomas, J. M. (1993). *Ultramicroscopy*, **49**, 198–209.

Schulze, G. E. R. (1934). *Z. Phys. Chem. B*, **24**, 215–240.

Schwarz, K. (1972). *Phys. Rev. B*, **5**, 2466–2468.

Schwitalla, J. & Ebert, H. (1998). *Phys. Rev. Lett.* **80**, 4586–4589.

Shirley, E. L. (1998). *Phys. Rev. Lett.* **80**, 794–797.

Shirley, E. L. (2000). *J. Electron. Spectrosc. Relat. Phenom.* **110–111**, 305–321.

Shirley, E. L. (2004). *J. Electron. Spectrosc. Relat. Phenom.* **136**, 77–83.

Šipr, O. (1996–1999). *rsms.* Institute of Physics AS CR, Prague, Czech Republic.

Šipr, O. (2002). *Phys. Rev. B*, **65**, 205115.

Šipr, O., Dalba, G. & Rocca, F. (2004). *Phys. Rev. B*, **69**, 134201.

Šipr, O., Rocca, F. & Dalba, G. (1999a). *J. Synchrotron Rad.* **6**, 770–772.

Šipr, O. & Šimůnek, A. (2001). *J. Phys. Condens. Matter*, **13**, 8519–8525.

Šipr, O., Šimůnek, A., Bocharov, S., Kirchner, T. & Dräger, G. (1999b). *Phys. Rev. B*, **60**, 14115–14127.

Šipr, O., Šimůnek, A. & Rocca, F. (2007). *AIP Conf. Proc.* **882**, 446–448.

Šipr, O., Šimůnek, A., Vackář, J., Dalba, G. & Rocca, F. (2006). *Phys. Chem. Glasses: Eur. J. Glass Sci. Technol. B*, **47**, 412–418.

Sugiyama, K. & Takeuchi, Y. (1985). *Z. Kristallogr.* **173**, 293–304.

Swinnea, J. S. & Steinfink, H. (1983). *Am. Mineral.* **68**, 827–832.

Vvedensky, D. D., Saldin, D. K. & Pendry, J. B. (1986). *Comput. Phys. Commun.* **40**, 421–440.

Yang, G., Möbus, G. & Hand, R. J. (2006). *Phys. Chem. Glasses: Eur. J. Glass Sci. Technol. B*, **47**, 507–512.

Zhang, G. P., Chang, G. S., Callcott, T. A., Ederer, D. L., Kang, W. N., Choi, E.-M., Kim, H.-J. & Lee, S.-I. (2003). *Phys. Rev. B*, **67**, 174519.